Quantitative imaging of ischemic stroke through thinned skull in mice with Multi Exposure Speckle Imaging

Ashwin B. Parthasarathy, S. M. Shams Kazmi and Andrew K. Dunn

Department of Biomedical Engineering, The University of Texas at Austin, Austin, TX 78712

ashwinbharadwaj@mail.utexas.edu

Abstract: Laser Speckle Contrast Imaging (LSCI) has become a widely used technique to image cerebral blood flow *in vivo*. However, the quantitative accuracy of blood flow changes measured through the thin skull has not been investigated thoroughly. We recently developed a new Multi Exposure Speckle Imaging (MESI) technique to image blood flow while accounting for the effect of scattering from static tissue elements. In this paper we present the first *in vivo* demonstration of the MESI technique. The MESI technique was used to image the blood flow changes in a mouse cortex following photothrombotic occlusion of the middle cerebral artery. The Multi Exposure Speckle Imaging technique was found to accurately estimate flow changes due to ischemia in mice brains *in vivo*. These estimates of these flow changes were found to be unaffected by scattering from thinned skull.

OCIS codes: (120.6150) Speckle imaging, (170.3890) Medical optics instrumentation, (170.0110) Imaging systems, (170.3880) Medical and biological imaging

References and links

1. A. Fercher and J. Briers, "Flow visualization by means of single-exposure speckle photography," Optics Communications **37**(5), 326–330 (1981).
2. A. Dunn, H. Bolay, M. Moskowitz, and D. Boas, "Dynamic Imaging of Cerebral Blood Flow Using Laser Speckle," Journal of Cerebral Blood Flow & Metabolism **21**, 195–201 (2001).
3. B. Weber, C. Burger, M. Wyss, G. von Schulthess, F. Scheffold, and A. Buck, "Optical imaging of the spatiotemporal dynamics of cerebral blood flow and oxidative metabolism in the rat barrel cortex," European Journal of Neuroscience **20**(10), 2664–2670 (2004).
4. T. Durduran, M. Burnett, G. Yu, C. Zhou, D. Furuya, A. Yodh, J. Detre, and J. Greenberg, "Spatiotemporal Quantification of Cerebral Blood Flow During Functional Activation in Rat Somatosensory Cortex Using Laser-Speckle Flowmetry," Journal of Cerebral Blood Flow & Metabolism **24**, 518–525 (2004).
5. D. Atochin, J. Murciano, Y. Gursoy-Ozdemir, T. Krasik, F. Noda, C. Ayata, A. Dunn, M. Moskowitz, P. Huang, and V. Muzykantov, "Mouse Model of Microembolic Stroke and Reperfusion," Stroke **35**(9), 2177–2182 (2004).
6. B. Ruth, "Measuring the steady-state value and the dynamics of the skin blood flow using the non-contact laser speckle method." Medical Engineering and Physics **16**(2), 105–11 (1994).
7. B. Choi, N. Kang, and J. Nelson, "Laser speckle imaging for monitoring blood flow dynamics in the in vivo rodent dorsal skin fold model," Microvascular Research **68**, 143–146 (2004).
8. K. Yaoeda, M. Shirakashi, S. Funaki, H. Funaki, T. Nakatsue, A. Fukushima, and H. Abe, "Measurement of microcirculation in optic nerve head by laser speckle flowgraphy in normal volunteers," American Journal of Opthalmology **130**(5), 606–610 (2000).
9. J. Briers, "Laser Doppler, speckle and related techniques for blood perfusion mapping and imaging," Physiological Measurement **22**, R35–R66 (2001).
10. D. Boas and A. Dunn, "Laser speckle contrast imaging in biomedical optics," Journal of Biomedical Optics **15**, 011,109 (2010).

#127521 - $15.00 USD Received 26 Apr 2010; revised 28 Jun 2010; accepted 1 Jul 2010; published 16 Jul 2010

11. R. Bandyopadhyay, A. Gittings, S. Suh, P. Dixon, and D. Durian, "Speckle-visibility spectroscopy: A tool to study time-varying dynamics," Review of Scientific Instruments **76**, 093,110 (2005).
12. A. Parthasarathy, W. Tom, A. Gopal, X. Zhang, and A. Dunn, "Robust flow measurement with multi-exposure speckle imaging," Optics Express **16**(3), 1975–1989 (2008).
13. R. Bonner and R. Nossal, "Model for laser Doppler measurements of blood flow in tissue," Applied Optics **20**(12), 2097–2107 (1981).
14. C. Ayata, A. Dunn, Y. Gursoy-Ozdemir, Z. Huang, D. Boas, and M. Moskowitz, "Laser speckle flowmetry for the study of cerebrovascular physiology in normal and ischemic mouse cortex," Journal of Cerebral Blood Flow & Metabolism **24**(7), 744–755 (2004).
15. H. Shin, A. Dunn, P. Jones, D. Boas, M. Moskowitz, and C. Ayata, "Vasoconstrictive neurovascular coupling during focal ischemic depolarizations," Journal of Cerebral Blood Flow & Metabolism **26**, 1018–1030 (2006).
16. H. Shin, P. Jones, M. Garcia-Alloza, L. Borrelli, S. Greenberg, B. Bacskai, M. Frosch, B. Hyman, M. Moskowitz, and C. Ayata, "Age-dependent cerebrovascular dysfunction in a transgenic mouse model of cerebral amyloid angiopathy," Brain **130**(9), 2310 (2007).
17. S. Yuan, A. Devor, D. Boas, and A. Dunn, "Determination of optimal exposure time for imaging of blood flow changes with laser speckle contrast imaging," Applied Optics **44**(10), 1823–1830 (2005).
18. S. J. Kirkpatrick, D. D. Duncan, and E. M. Wells-Gray, "Detrimental effects of speckle-pixel size matching in laser speckle contrast imaging," Optics Letters **33**(24), 2886–2888 (2008).
19. D. D. Duncan and S. J. Kirkpatrick, "Can laser speckle flowmetry be made a quantitative tool?" J. Opt. Soc. Am. A **25**(8), 2088–2094 (2008).
20. P. Li, S. Ni, L. Zhang, S. Zeng, and Q. Luo, "Imaging cerebral blood flow through the intact rat skull with temporal laser speckle imaging," Optics Letters **31**(12), 1824–1826 (2006).
21. P. Zakharov, A. Völker, A. Buck, B. Weber, and F. Scheffold, "Quantitative modeling of laser speckle imaging," Opt. Lett. **31**(23), 3465–3467 (2006).
22. P. Zakharov, A. V
"olker, M. Wyss, F. Haiss, N. Calcinaghi, C. Zunzunegui, A. Buck, F. Scheffold, and B. Weber, "Dynamic laser speckle imaging of cerebral blood flow," Opt. Express **17**, 13,904–13,917 (2009).
23. W. Tom, A. Ponticorvo, and A. Dunn, "Efficient Processing of Laser Speckle Contrast Images," IEEE Transactions on Medical Imaging **27**(12), 1728–1738 (2008).
24. P. Lemieux and D. Durian, "Investigating non-Gaussian scattering processes by using n th-order intensity correlation functions," Journal of Optical Society of America A **16**(7), 1651–1664 (1999).
25. D. Boas and A. Yodh, "Spatially varying dynamical properties of turbid media probed with diffusing temporal light correlation," Journal of Optical Society of America A **14**(1), 192–215 (1997).
26. B. Watson, W. Dietrich, R. Busto, M. Wachtel, and M. Ginsberg, "Induction of reproducible brain infarction by photochemically initiated thrombosis," Annals of neurology **17**(5), 497–504 (1985).
27. J. Lee, M. Park, Y. Kim, K. Moon, S. Joo, T. Kim, J. Kim, and S. Kim, "Photochemically induced cerebral ischemia in a mouse model," Surgical neurology **67**(6), 620–625 (2007).
28. C. Cheung, J. Culver, K. Takahashi, J. Greenberg, and A. Yodh, "In vivo cerebrovascular NIRS measurement," Physics in Medicine and Biology **46**, 2053–2065 (2001).
29. T. Durduran, C. Zhou, B. Edlow, G. Yu, R. Choe, M. Kim, B. Cucchiara, M. Putt, Q. Shah, S. Kasner, *et al.*, "Transcranial optical monitoring of cerebrovascular hemodynamics in acute stroke patients," Opt. Express **17**, 3884–3902 (2009).

1. Introduction

Laser Speckle Contrast Imaging (LSCI) is a minimally invasive optical technique to image blood flow *in vivo*. The primary advantage of LSCI is that blood flow measurements can be obtained at high spatial and temporal resolutions using inexpensive and relatively simple instrumentation. For these reasons, since being first implemented for biological applications by Fercher and Briers[1], LSCI has been used extensively to image blood flow in the brain [2, 3, 4, 5], skin [6, 7] and retina [8]. A few recent reviews [9, 10] have outlined the basic principles of laser speckle and some of its most popular applications.

Briefly, speckle is caused by the coherent addition of randomly scattered laser light. The scattered photons travel slightly different paths and interfere at the detector, which in the case of LSCI is a camera sensor, to produce a grainy pattern. When the photons scatter off moving particles, they cause temporal fluctuations in the speckle pattern [1, 10]. These fluctuations can be easily converted to spatial contrast, by computing the ratio of the standard deviation to the mean intensity in a local region [2]. This speckle contrast is then related to the exposure duration

#127521 - $15.00 USD Received 26 Apr 2010; revised 28 Jun 2010; accepted 1 Jul 2010; published 16 Jul 2010

of the camera (T) and the correlation time (τ_c) using mathematical models [1, 11, 12]. More accurately, τ_c is the characteristic decay time of the backscattered speckle electric field [12, 1, 11]. The final measure of blood flow with LSCI is hence the correlation time (τ_c), which follows an inverse relationship to blood flow [13]. While the absolute value of blood flow in terms of m/sec is very difficult to determine, correlation time measures and relative correlation time measures are acceptable measures of blood flow[14].

The basic LSCI technique has been largely unchanged from its original form [1, 9]. Consequently, many of its limitations still remain. For example, the LSCI technique is good at measuring relative changes in blood flow, but cannot produce baseline measures. Additionally, LSCI may underestimate large decreases in flow, particularly in the presence of static scatterers [12]. It is important to correct this underestimation in large flow changes for applications such as mapping the effects of stroke in the brain, where tissue viability is often estimated from the spatial extent of reduction in blood flow [2, 15, 14]. Another limitation has been the inability of LSCI to account for scattering from static tissue elements, such as the skull. While this limitation can be overcome by performing a full craniotomy, it is preferable to retain at least a thinned skull for chronic and long term studies [16]. Furthermore, in other areas of application such as blood flow measurement in the skin, it is not always feasible to physically remove the static scattering components.

There has been some recent progress in improving the theory and instrumentation of LSCI. Yuan et. al. [17] described some basic instrumentation details which help increase sensitivity of LSCI to flow changes, while recently Kirkpatrick et. al. [18] described practical conditions that would help reduce errors in computing speckle contrast. Bandyopadhyay et. al. [11] corrected what had been a persistent mathematical error in the model describing speckle contrast. Duncan et. al. [19] presented some arguments on the proper statistical model to be used in describing speckle contrast. Some progress has been made in accounting for the presence of static tissue elements. Li et. al. [20] showed that blood flow measurements can be made through the skull using a temporal processing scheme. Zakharov et. al. [21] presented a mathematical model to account for the presence of static particles and later [22] presented a refined processing technique to obtain cerebral blood flow measurements through the thin skull.

Recently, we presented an improved speckle imaging technique called Multi Exposure Speckle Imaging (MESI) that takes advantage of the dependence of the speckle contrast on camera exposure duration and addresses some of the limitations mentioned here [12]. We developed a new mathematical model to account for the presence of static tissue elements, and a new instrument to utilize this model and produce accurate and consistent measures of blood flow changes in the presence of static scatterers using flow phantoms. In this paper, we show that the MESI technique works well *in vivo*, by imaging blood flow changes induced by occluding the middle cerebral artery (MCA) in a mouse brain. We show that our technique accurately predicts an almost 100% reduction in blood flow due to the stroke. Also, using a partial craniotomy model, we demonstrate that MESI estimates of blood flow changes are not affected by the presence of a thin skull.

2. Materials and Methods

2.1. The Multi Exposure Speckle Imaging technique

The Multi Exposure Speckle Imaging (MESI) instrument is shown in Figure 1a. Speckle images at different camera exposure durations are acquired by triggering a camera (Basler 602f, Basler Vision Technologies, Germany) and simultaneously gating a laser diode ($\lambda = 660$nm, 95mW, Micro laser Systems Inc., Garden Grove, CA, USA) with an acousto optic modulator to equalize the energy of each laser pulse. The first diffraction order is directed towards the animal, and the backscattered light is collected by a microscope objective ($10X$) and imaged onto the cam-

#127521 - $15.00 USD Received 26 Apr 2010; revised 28 Jun 2010; accepted 1 Jul 2010; published 16 Jul 2010

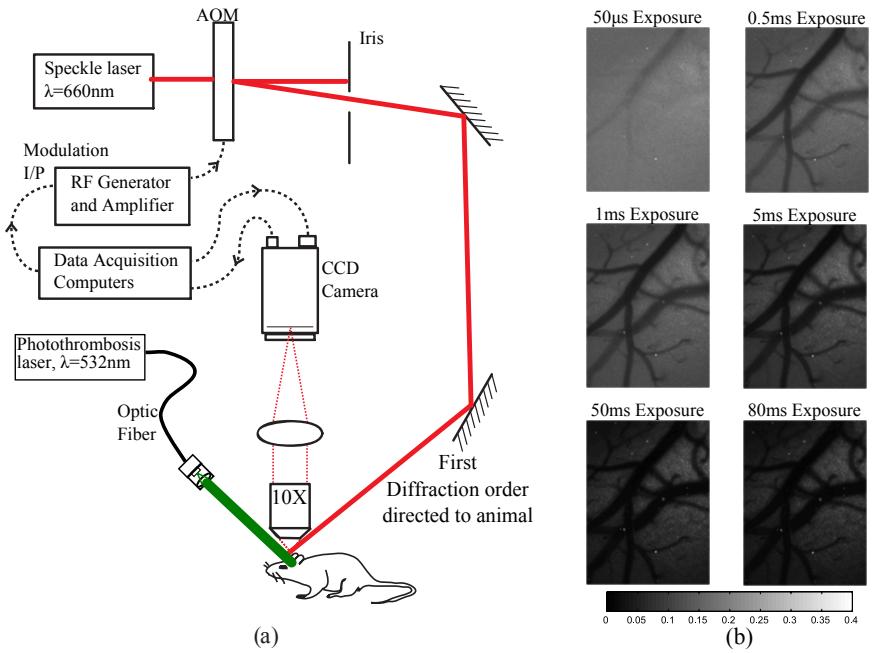

Fig. 1. (a) Schematic of the Multi Exposure Speckle Imaging (MESI) instrument, adapted from our previous publication [12] (b) Representative speckle contrast images of mouse cortex obtained at various camera exposure durations using the MESI instrument

era. By appropriately controlling the acousto-optic modulator, the intensity of light in the first diffraction order and hence the average intensity recorded by camera is maintained a constant over different exposure durations [12]. More information about the instrument is available in our previous publication [12]. Laser speckle images were collected at 15 different exposure durations from 50μs to 80ms, and the entire setup was controlled by custom software [23]. Spatial speckle contrast images was computed using a window size of $N = 7$. Figure 1b shows some speckle contrast images of the mouse cortex at different camera exposure durations. While this is not the first *in vivo* demonstration of speckle images at multiple exposure durations [17], we note that these images span almost 3 orders of magnitude of exposure duration which is possible with an inexpensive camera using the MESI approach.

The Multi Exposure Speckle Imaging (MESI) technique involves the use of the MESI instrument (Figure 1a) in conjunction with a mathematical model that relates the speckle contrast to the camera exposure duration, T and the decay time of the speckle autocorrelation function,τ_c. In our previous publication [12], we derived and validated a robust speckle model (Equation 1), building on previous work done by Bandyopadhyay et. al. [11] and Lemieux et. al. [24]. This model is designed to account for the heterodyne mixing [24] of light scattered from static and moving particles, as well as the contributions of nonergodic light and experimental noise to speckle variance.

$$K(T,\tau_c) = \left\{ \beta\rho^2 \frac{e^{-2x}-1+2x}{2x^2} + 4\beta\rho\,(1-\rho)\,\frac{e^{-x}-1+x}{x^2} + v_{ne} + v_{noise} \right\}^{1/2}, \qquad (1)$$

where $x = \frac{T}{\tau_c}$, $\rho = \frac{I_f}{(I_f+I_s)}$ is the fraction of total light that is dynamically scattered, β is a normalization factor to account for speckle averaging effects, T is the camera exposure duration, τ_c

#127521 - $15.00 USD Received 26 Apr 2010; revised 28 Jun 2010; accepted 1 Jul 2010; published 16 Jul 2010

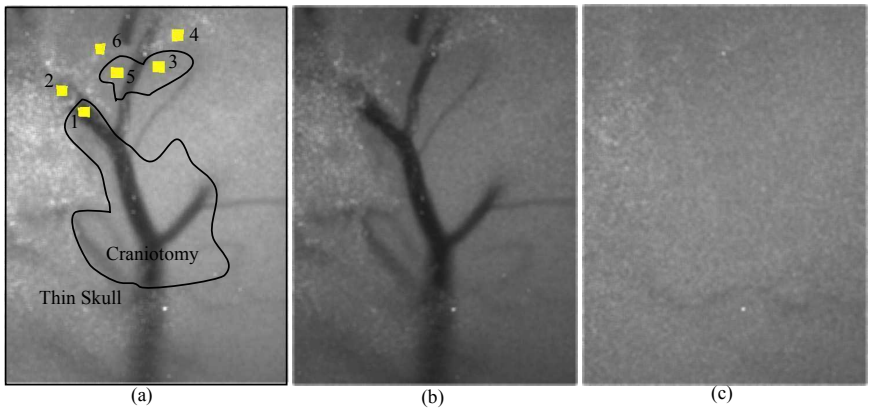

Fig. 2. (a) Speckle contrast image (5ms exposure duration) illustrating the partial craniotomy model. The regions within the closed loops (Regions 1, 3 and 5) are in the craniotomy. Regions outside the closed loops (Regions 2, 4 and 6) are in the thin skull region. Speckle Contrast images of a branch of the MCA, illustrating ischemic stroke induced using photo thrombosis (b) Before stroke (c) After stroke

the correlation time is the characteristic decay time of the speckle electric field autocorrelation function, v_{noise} is the constant variance due to experimental noise and v_{ne} is the constant variance due to nonergodic light. For our experiments, we lump v_{noise} and v_{ne} into a single spatial variance $v_s = v_{ne} + v_{noise}$. v_{ne} in Equation 1 is a constant that is used to link spatial speckle analysis with temporal statistics. The exact value of the constant and its mathematical expression does not affect the flow estimates. However it can be derived using Equation 16 from Boas et. al. [25]. The MESI data, which consists of speckle contrast measurements obtained at multiple exposure durations using the instrument (Figure 1a) can now be fit to Equation 1 to find unknown constants β, ρ, v_s, and τ_c which is a measure of flow. The ability to experimentally measure speckle variance as a function of exposure duration of the camera, enables better and more consistent estimates of τ_c and hence blood flow.

2.2. Animal preparation

The MESI technique was used to image cerebral blood flow changes that occur during ischemic stroke in mice. Mice (CD-1; male, $25-30$ g, n $= 5$) were used for these experiments. All experimental procedures were approved by the Animal Care and Use Committee at the University of Texas at Austin. The animals were anesthetized by inhalation of $2-3\%$ isoflurane in oxygen through a nose cone. Body temperature was maintained at 37^{o}C using a feedback controlled heating plate (ATC100, World Percision Instruments, Sarasota, FL, USA) during the experiment. The animals were fixed in a stereotaxic frame (Kopf Instruments, Tujunga, CA, USA) and an ~ 3mm $\times$ 3mm portion of the skull was exposed by thinning it down using a dental burr (Ideal^{TM} Micro-Drill, Fine Science tools, Foster City, CA, USA). Further, part of this thinned skull was removed to create a partial craniotomy (shown in Figure 2a). Care was taken to ensure that the boundary between the thin skull and the craniotomy was over a vessel and that the boundary was away from major branches. This ensured that one can expect the same blood flow changes across the boundary. The partial craniotomy was completed by building a well around the region using dental cement and filling it with mineral oil. The surgery was supplemented with subcutaneous injections of Atropine (0.04mg/kg) every hour to prevent respiratory difficulties and intraparetonial injections of dextrose-saline (2ml/kg/h of 5%w/v) for hydration.

#127521 - $15.00 USD Received 26 Apr 2010; revised 28 Jun 2010; accepted 1 Jul 2010; published 16 Jul 2010

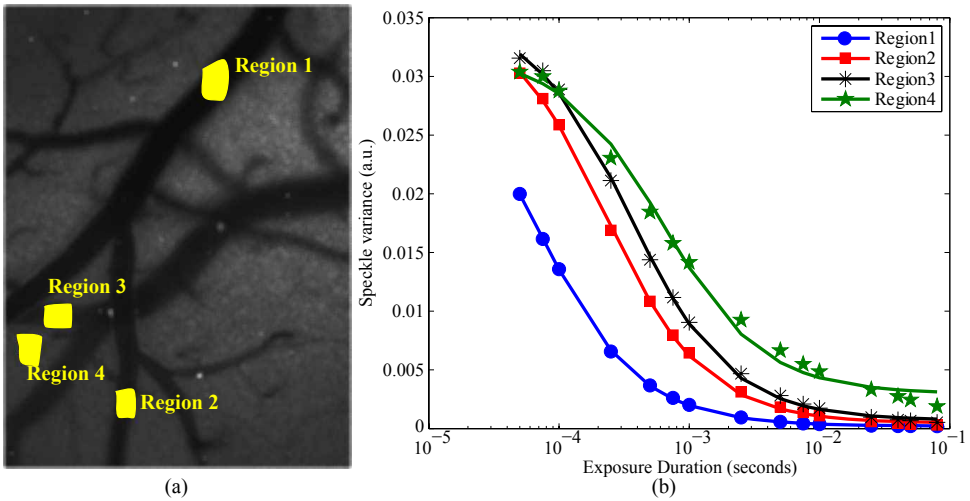

Fig. 3. (a) Speckle contrast image (5ms exposure) illustrating regions of different flow (b) Time integrated speckle variance curves with decay rates corresponding to flow rates. The data points have been fit to Equation 1

2.3. *Ischemic stroke using photothrombosis*

To induce an ischemic stroke, the middle cerebral artery (MCA) was occluded using photothrombosis [26, 27]. During animal preparation, the temporalis muscle in the same hemisphere of the craniotomy was carefully resected from the temporal bone. The temporal bone was then thinned using the dental burr till it was transparent and the MCA was visible. A laser beam ($\lambda = 532$nm, Spectra Physics, Santa Clara, CA, USA) was directed towards the MCA through an optical fiber. Typical laser power delivered to the animal during the experiment was $\sim 0.5 - 0.75$W. During the experiment, a 1ml bolus intraparetonial injection of a photo sensitive thrombotic agent Rose Bengal (15mg/kg) was administered to the animal. The laser light interacts with the Rose Bengal to cause thrombosis in the MCA resulting in occlusion. Figures 2b & c show LSCI images (at 5ms exposure) before and after the stroke was induced. Occluding the MCA created a severe stroke and reduced blood flow by almost 100% in the cortical regions downstream.

2.4. *Imaging paradigm*

The experimental setup shown in Figure 1 was used to acquire multi exposure speckle images before, during and after the stroke. Laser speckle images at 15 exposure durations ranging from 50μs to 80ms were used to compile one MESI frame. Typically, 3000 MESI frames were collected for each experiment. Each MESI frame took ~ 1.5 seconds to acquire. The field of view of the cortex as measured by the MESI instrument was $\sim 800 \times 500\mu$m. Specific regions of interest as shown in Figure 3a were identified, and the average speckle contrast in these regions were computed for all MESI frames to produce the time integrated speckle contrast curves shown in Figure 3b. Each curve was then fit to Equation 1 to estimate blood flow (τ_c).

#127521 - $15.00 USD Received 26 Apr 2010; revised 28 Jun 2010; accepted 1 Jul 2010; published 16 Jul 2010

3. Results

3.1. *Estimating blood flow using the MESI technique*

Figure 3 illustrates the first step in obtaining blood flow estimates using the MESI technique. In this example, the MESI instrument (Figure 1a) was used to obtain raw speckle images at multiple exposure durations of a mouse brain whose cortex had been exposed by performing a full craniotomy. After converting these raw images to speckle contrast images, specific regions of interest were identified (Figure 3a), and the average speckle contrast in these regions were computed and plotted as a function of camera exposure duration (Figure 3b). These experimentally measured time integrated speckle variance, $K(T,\tau_c)^2$ curves were then fit to Equation 1 using the `Trust-Region` algorithm to obtain estimates for blood flow (through τ_c, the decay time of the speckle autocorrelation function [12, 14]). The curves correspond to different regions shown in Figure 3a. From these curves, it can be observed that the variance decays with a lower τ_c value (and hence higher blood flow) in region 1 which is in the middle of a major vessel (a vein), when compared to region 4 which is in the parenchyma.

3.2. *Imaging blood flow changes due to ischemic stroke*

For stroke experiments, the partial craniotomy procedure was followed during animal preparation. A representative image of this model is shown in Figure 4a. Regions 1, 3, and 5 are in the craniotomy, while regions 2, 4 and 6 are under the thin skull. MESI images were obtained and the blood flow was estimated using the procedures described in the previous section. Figure 4b shows how the time integrated speckle variance curves are different for two regions across the thin skull boundary. The primary points of difference between the curves obtained from regions across the boundary are (a) an apparent change in the shape of the time integrated speckle vari-

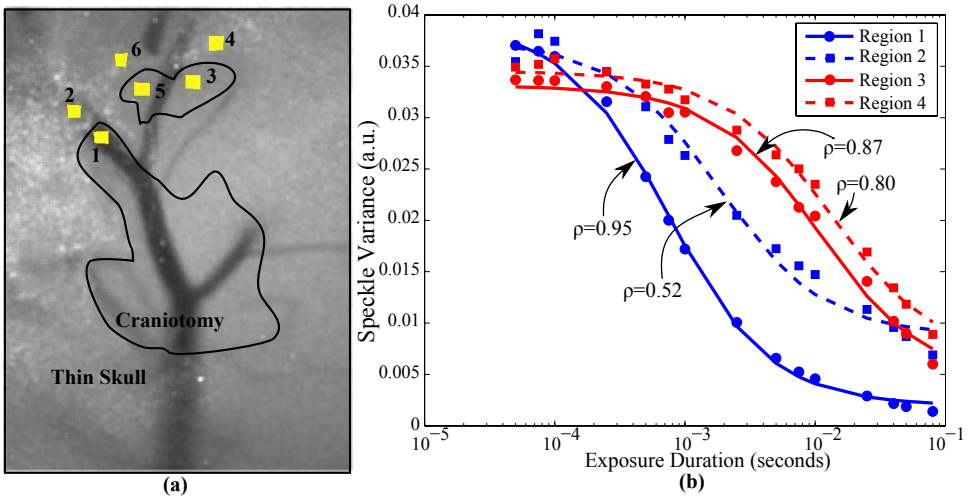

Fig. 4. (a) Illustration of partial craniotomy model. The regions enclosed by the closed loops (regions 1, 3 & 5) are located in the craniotomy. Regions outside of the closed loops (regions 2, 4 & 6) are located in the thinned (but intact) skull. (b) Time integrated speckle variance curves illustrating the influence of static scattering due to the presence of the thinned skull. A decrease in the value of ρ indicates an increase in the amount of static scattering. Regions 2 and 4 show distinct offset at large exposure durations. This offset it due to increased v_s over the thinned skull

#127521 - $15.00 USD Received 26 Apr 2010; revised 28 Jun 2010; accepted 1 Jul 2010; published 16 Jul 2010

ance curve over the thin skull due to variation in ρ (the fraction of light that is dynamically scattered [12]), and (b) an increase in the variance at the longer exposure durations due to an increase in v_s (the constant spatial variance that accounts for nonergodicity and experimental noise [12]). This difference is more apparent in the regions on the vessel (regions 1 and 2) than it is in regions in the parenchyma (regions 3 and 4). With LSCI at a single exposure, regions 1 and 2 measure vastly different speckle contrast values even though the actual blood flow is likely identical. Under baseline conditions, the ratio of the correlation time in region 1 to the correlation time in region 2 was found to be 0.6238 ± 0.0238 using the MESI technique, while this ratio was estimated to be 0.3771 ± 0.0215 using the LSCI technique. While the ideal value for these ratios should be 1, these estimates suggest that the MESI technique predicts τ_c values that are more consistent across the thin skull boundary. The ratio of the correlation time in region 3 to the correlation time in region 4 was found to be 0.883 ± 0.055 using the MESI technique, while this ratio was estimated to be 0.889 ± 0.019 using the LSCI technique. The MESI and LSCI estimates of these ratios are similar over the parenchyma regions because the thickness of the thinned skull is nonuniform and was found to be thinner, as evidenced by higher values of ρ in region 4 compared to region 2.

Each stroke experiment was performed after waiting for about 30 minutes after surgical preparation. The first 10 minutes of the data was used as baseline measures to compute the relative blood flow change. The thrombosis inducing laser was kept on during the entire course of the experiment. Rose Bengal was injected 10 minutes after start of the experiment and data collection was continued for about an hour. Data acquisition was not stopped while the dye was being injected. Immediately after the completion of data acquisition, the animal ($n = 2$) was sacrificed and 30 MESI frames (1 MESI frame consists of 15 exposure durations) were collected as a zero flow reference.

Since β is an experimental constant, its *in vivo* determination is important to obtain accurate flow measures [12]. In addition to β, ρ and v_s also have to be determined *in vivo*. However, we contend that changes in the physiology can change ρ and v_s, and hence these parameters were not held fixed during the fitting process. First, β was estimated under baseline conditions for the regions in the craniotomy (regions 1, 3 and 5 shown in figure 4a), by using equation 1 and holding $\rho = 1$. A statistical average of the estimated values of β were found for each region and this average value was used for the corresponding pair. For example, the value of β estimated from region 1, would be used for regions 1 and 2. The MESI curves from entire data set was then fit to Equation 1 using the estimated value of β, and holding it constant. Unknown parameters ρ, v_s and the flow measure τ_c were estimated from this fitting process.

Figure 5a shows the relative blood flow change as measured using the MESI technique in region 1, in the same animal as in Figure 4. Since τ_c can be assumed to be inversely related to blood flow [13], relative blood flow may be defined as the ratio of $\tau_{baseline}$ to $\tau_{measured}$. Here, $\tau_{baseline}$ is the statistical average of the correlation time estimates during the first 10 minutes. From time $t = 10$ min to $t = 30$ min, the blood flow is seen to fluctuate. These fluctuations are due to the increase and decrease of blood flow while the clot is being formed in the MCA. For the MCA to be completely occluded, the photo thrombosis process has to create enough thrombus to occlude the vessel and its downstream branches. Since the MCA is a major artery, partially formed thrombus can be washed down by blood pressure. The partially formed clots break down and produce blood flow fluctuations. These fluctuations were observed in all animals before the stroke was formed. Once the thrombosis process is complete, the blood flow settles to a stable value. Figure 5a shows that the relative blood flow drops to almost 0 after the clot is fully formed. The average percentage reduction in blood flow in the blood vessel, due to the ischemic stroke in all animals was estimated to be $97.3 \pm 2.09\%$ using the MESI technique and $87.67 \pm 7.04\%$ using the LSCI technique. The estimates of average percentage reduction in

#127521 - $15.00 USD Received 26 Apr 2010; revised 28 Jun 2010; accepted 1 Jul 2010; published 16 Jul 2010

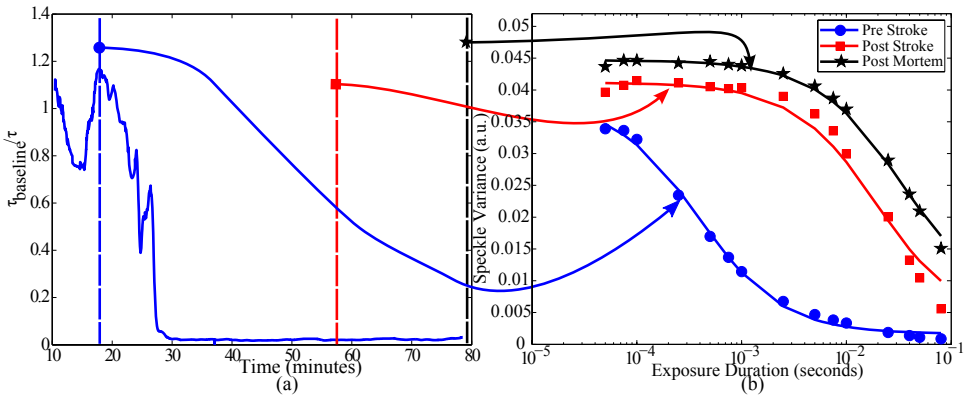

Fig. 5. Relative blood flow change caused due to the ischemic stroke in the branch of the MCA (Region 1 in Figure 4a). (a) Time course of relative blood flow change in Region 1 as estimated using the MESI technique. The flow estimates in first 10 minutes were considered as baseline. The reduction in blood flow due to the stroke, is estimated to be $\sim 100\%$, which indicates that blood supply to the artery has been completely shut off. (b) MESI curves illustrating the change in the shape of the curve as blood flow decreases. The MESI curve obtained after the stroke is found to be similar in shape to that obtained after the animal was sacrificed. This is a qualitative validation of $\sim 100\%$ decrease in blood flow in the artery

blood flow obtained using the MESI technique were found to be statistically greater than those obtained using the LSCI technique with a 5% significance level.

In Figure 5b, we show three representative time integrated speckle variance curves estimated from region 1 (Figure 4a) as a function of camera exposure duration, illustrating the progression of the stroke in one representative animal. The first two curves are the time integrated speckle variance curves before and after ischemic stroke. The drastic change in the shape of the curve reinforces the observation that the change in blood flow is drastic, as previously noted in Figure 2 and Figure 5a. The shape of the curve after the stroke has been induced is indicative of Brownian motion. This trend was observed in all animals, and is comparable to similar measurements in literature [12, 11]. An experimental measurement of the time integrated speckle variance curve after the animal has been sacrificed (comparing the blue and black curves in Figure 5b) further confirm these observations. In region 1 we estimated the average percentage reduction in blood flow due to death in all animals to be about 99% using the MESI technique and 92% using the LSCI technique. Since after death, the blood flow in the animals should be zero, we conclude that the MESI technique has greater accuracy in predicting large flow decreases. This observation is consistent with our previous measurements in phantoms [12].

While the post stroke and post mortem time integrated speckle variance curves are similar, the variances are different. The increase in measured speckle variance after the animal has been sacrificed is indicative of a further drop in blood flow. This drop is measured as a mild increase in τ_c. One of the reasons for the difference in speckle variance between the post stroke and the post mortem cases, is that in the post stroke case, the speckle contrast can still be affected by blood flow from deeper tissue regions (though not spatially resolved) which could possibly be unaffected by thrombosis. Additionally, the pulsation of the cortex in a live animal contributes to a reduction in variance. In the post mortem case, this pulsation is absent, and the blood flow is truly zero over the entire cortex. The only motion we detect is due to limited (thermal induced) Brownian motion that can be associated with the dead cells. These factors coupled

#127521 - $15.00 USD Received 26 Apr 2010; revised 28 Jun 2010; accepted 1 Jul 2010; published 16 Jul 2010

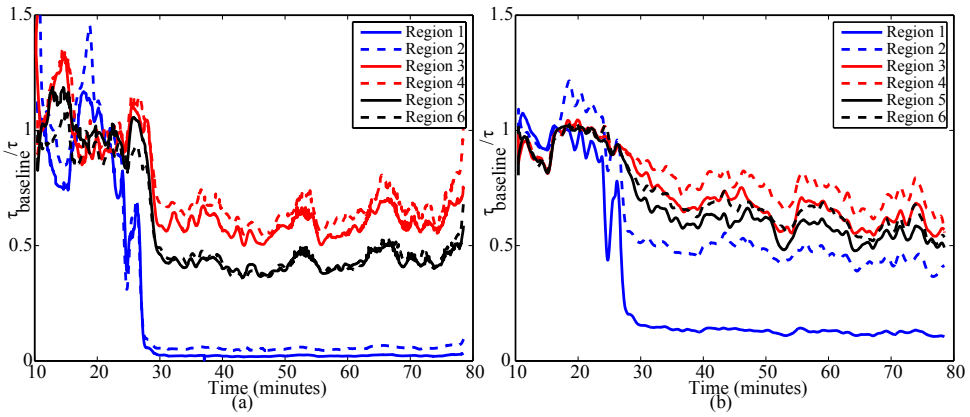

Fig. 6. MESI technique can predict consistent blood flow changes across the thin skull - craniotomy boundary. (a) Relative blood flow changes estimated using the MESI technique in 3 pairs of regions across the boundary (Figure 4a). The change in blood flow is found to be similar for each pair of regions. (b) Relative blood flow changes estimated using the LSCI technique (at 5ms exposure) in 3 pairs of regions across the boundary (Figure 4a). The change in blood flow is not similar for each pair of regions. This difference is especially prominent over the vessel (Regions 1 and 2)

with physiological noise contribute to the difference in variance between the post mortem and the post stroke cases. From these observations, we conclude that the magnitude of the blood flow reduction measured by the MESI technique is accurate.

3.3. Imaging blood flow changes through the thin skull

Figure 6 compares the relative blood flow measures as estimated by (a) MESI technique and (b) LSCI technique at 5ms exposure duration. 5ms exposure duration was selected for comparison because it has been demonstrated to be sensitive to blood flow changes *in vivo* [17]. Considering the first pair of regions across the thin skull boundary (regions 1 and 2 in Figure 4a), the relative blood flow measures as estimated by the MESI technique (solid and dashed blue lines in Figure 6a) were found to be similar. The estimates of relative blood flow measures obtained using the MESI technique were found to be statistically similar in 10 locations across the thin skull. This indicates that the relative blood flow measures obtained using the MESI technique are unaffected by the presence of the thin skull. The LSCI estimates (Figure 6b) however show two significant differences. One, the relative blood flow estimate for region 1 is not close to 0 after the stroke, but is rather close to 0.2 and two, the relative blood flow measures across the boundary (solid and dashed blue lines in Figure 6b) are different. The first observation is an *in vivo* reproduction of LSCI's underestimation of large flow changes we reported in an earlier publication [12], and the second observation is the very limitation that the MESI technique is designed to overcome. The estimates of relative blood flow measures obtained using the LSCI technique were not found to be statistically similar in 10 locations across the thin skull.

These observations can also be made in relative blood flow measures from the other two pairs of regions, regions 3 & 4 and regions 5 & 6, both in the parenchyma. In these regions we see a similar trend, but the difference between the two techniques is not as drastic as it is in the blood vessel. Typically, each pixel in the image samples a large distribution of blood flows. The statistical models we use to describe speckle contrast assume that there is one value of blood flow (and hence one τ_c) in the sampling volume. This assumption is more valid over large blood

#127521 - $15.00 USD Received 26 Apr 2010; revised 28 Jun 2010; accepted 1 Jul 2010; published 16 Jul 2010

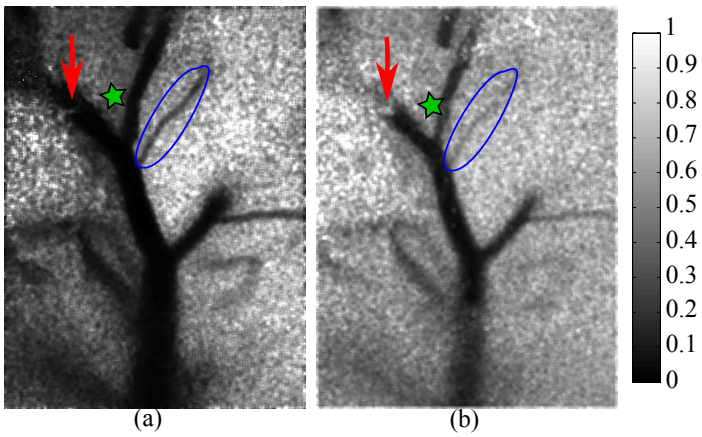

Fig. 7. Full field relative correlation time maps obtained using the (a) MESI technique (b) LSCI technique (5ms exposure). Three corresponding regions marked in the figures illustrate the superior performance of the MESI technique. The boundary (corresponding to the boundary between the thin skull and the craniotomy) indicated by the red arrow is clearly visible in (b), but not in (a). There is a clear change gradient in the region indicated by the star in (b), but this gradient is invisible in (a). The vessel circled is more visible in (a) compared to (b). Relative correlation time estimates obtained using the MESI technique are not affected by the presence of thinned skull. Hence, similar estimates of blood flow changes are obtained across the boundary between the thin skull and craniotomy regions, leading to the absence of any gradients in blood flow change in (a)

vessels (or in a microfluidic phantom [12]), where there is a clear direction and rate, for flow. However in the parenchyma, the photons can sample a larger distribution of blood flow rates and we measure a statistical average of these different flow rates. It should be noted that this limitation is common to any dynamic light scattering based measurement. For these reasons, the MESI measurements are likely to be more accurate over the large blood vessel than the parenchyma. We still notice that the MESI estimates of relative flow are more consistent than the LSCI estimates, and that the MESI technique estimates a larger reduction in blood flow.

Figure 7 provides a full field perspective of the relative blood flow changes. These are full field maps of the relative correlation time, computed by taking the ratio of τ_c under baseline conditions to τ_c at a single time point after the stroke, as estimated using the MESI technique (Figure 7a) and the LSCI technique at 5ms exposure duration (Figure 7b). Both images are displayed on a scale of 0 to 1. The thin skull boundary is clearly visible in the LSCI estimate (Figure 7b), while the demarcation between the craniotomy and the thin skull is less obvious in the MESI estimates (Figure 7a). This difference is illustrated in the figures using (1) a red arrow and (2) a green star. Additionally, we see that some vessels are more visible in the MESI estimate. One example of this is illustrated by the blue oval. These images show that the MESI technique is better in estimating relative blood flow than LSCI and that these estimates are not affected by the presence of a thin skull. Additionally, the vessels in Figure 7a appear larger because the blood flow is better resolved using the MESI technique.

4. Discussion

The change in the shape of the time integrated speckle variance curves due to the presence of static tissue elements is consistent with our previous measurements in flow phantoms [12].

#127521 - $15.00 USD Received 26 Apr 2010; revised 28 Jun 2010; accepted 1 Jul 2010; published 16 Jul 2010

While in the case of the tissue phantoms, the change in the shape was affected in equal parts due to the influence of ρ and v_s, in the *in vivo* measures, we find that the static speckle variance v_s is the more dominant factor. In the microfluidic device we used earlier, the flow channel was the only part of the device containing dynamic scatterers. We believe that in the microfluidic device, the influence of ρ was greater due to the opportunity for a photon to interact with static particles on the sides of the channel and below the channel. This is clearly not the case *in vivo*, because the only place where a photon can interact from a static particle is from the thin skull. This could explain a comparatively reduced role that ρ plays in the *in vivo* measurements. Nevertheless, there is no way of accurately determining the value of ρ or v_s without using Equation 1 and the MESI instrument. Hence, the MESI technique is better suited to obtain consistent and accurate measurements of blood flow changes in the presence of a thin skull. Our technique is similar to the methods used by Zakharov et. al. [22], who presented an alternate method to estimate blood flow accurately in the presence a thinned skull. While their dynamic Laser Speckle Imaging technique aims at separating the dynamic speckle fluctuations from the static component, our MESI technique is aimed at interpreting and modeling the recorded intensity as a mixture of temporal and static back scattered intensities.

Recently, Duncan et. al. [19] pointed out that a Gaussian function ($g_1(\tau) = e^{-\tau^2/\tau_c^2}$) is a better statistical model to describe the dynamics of ordered flow in a vessel as opposed to the traditionally used negative exponential model [1] ($g_1(\tau) = e^{-\tau/\tau_c}$). The former corresponds to a Gaussian distribution of velocities, while the negative exponential model corresponds to a Lorentzian distribution of velocities in the sample volume. In order to test this hypothesis, we proceeded to derive a new MESI expression using the Gaussian function to describe speckle dynamics, and account for scattering from static tissue elements. We substituted $g_1(\tau) = e^{-\tau^2/\tau_c^2}$ in Equation 9 in our previous publication [12] and evaluated the integral to arrive at the new expression.

$$K(T,\tau_c) = \left\{ \beta\rho^2 \frac{e^{-2x^2} - 1 + \sqrt{2\pi}x\,\mathrm{erf}(\sqrt{2}x)}{2x^2} + 2\beta\rho(1-\rho)\frac{e^{-x^2} - 1 + \sqrt{\pi}x\,\mathrm{erf}(x)}{x^2} + v_{ne} + v_{noise} \right\}^{1/2}, \quad (2)$$

We estimated the relative blood flow changes in regions 1 and 2 (Figure 4a) using Equation 2 and the MESI technique. We compared these estimates to those we already obtained using Equation 1 and to the corresponding LSCI estimates at a few exposure durations other than 5ms. These results are plotted in Figure 8.

From Figure 8 we observe that using the Gaussian statistical model and Equation 2 do not change our estimates of relative flow *changes* significantly. By incorporating the principles of heterodyne mixing into Equation 2 and by using the MESI technique, we are still able to obtain consistent flow measures across the boundary of the thin skull. Duncan et. al [19] also pointed out that the differences between the Lorentzian and the Gaussian models are more prominent at the lower exposure durations. By sampling a range of exposure durations, we are minimizing the difference between the two models. Also as we explained earlier, each speckle samples a wide range of flow rates. The differences between the two models are not significant enough to overcome the statistical variability in value of τ_c. In addition, physiological noise and variability are bigger sources of uncertainty in the fitting process than a small change affected by using a different model. Our observations are in agreement with Cheung et. al [28] and Durduran et. al. [29] who showed that the Lorentzian model is a better fit for *in vivo* blood flow measurements using noninvasive diffuse correlation spectroscopy measurements, due to the complex fluid dynamics of blood flow in vessels.

#127521 - $15.00 USD Received 26 Apr 2010; revised 28 Jun 2010; accepted 1 Jul 2010; published 16 Jul 2010

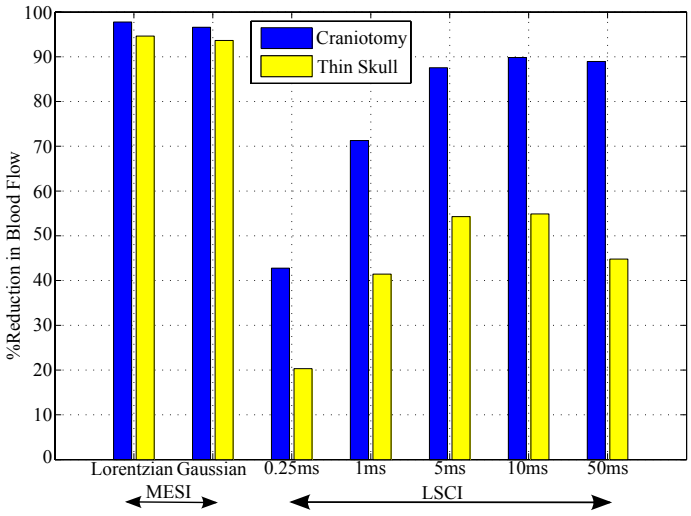

Fig. 8. Comparison of the percentage reduction in blood flow obtained in regions 1 and 2 (Figure 4a) using the MESI technique using two different speckle expressions (Lorentzian: Equation 1 and Gaussian: Equation 2) and multiple single exposure LSCI estimates. MESI estimates are found to be more consistent in estimating blood flow decreases across the boundary between the thin skull and the craniotomy. There is significant difference between the two models in estimating blood flow decrease

In Figure 8, while comparing the LSCI estimates of relative blood flow decrease at multiple exposure durations, we observe that at 5ms the percentage reduction in blood flow is about 10% lower than those obtained with the MESI technique. We also observe that the choice of exposure time in LSCI can drastically change the estimated blood flow reduction. For example, at 1 ms (another popular choice for *in vivo* measurements), LSCI predicts a 70% drop in blood flow due to stroke, which is almost 30% lower than the MESI estimates. This is not surprising because the sensitivity to change in blood flow has previously been shown to depend on the choice of exposure duration [17]. This is another reason why the LSCI estimates did not completely pick up the drop in blood flow in a small vessel circled in Figures 7a & b. It is hence impossible to accurately measure with a single exposure duration, the change in blood flow of all vessels in a field of view that consists of vessels of different diameters (and hence different blood flows). Also, we note that the estimates of relative blood flow changes are not consistent across the thin skull boundary for any of the single exposure measurements. From this we can conclude that for experiments where a relatively small change in blood flow is expected, the LSCI technique may be adequate, provided the sample is free from static tissue elements and the right choice of exposure duration is made before the experiment. For imaging large changes in blood flow or for imaging samples where dynamic and static scatterers are mixed, the MESI technique is likely to yield more accurate estimates of flow changes.

5. Conclusion

In this paper we have addressed two of the major limitations of the Laser Speckle Contrast Imaging technique to measure cerebral blood flow. By using a new Multi Exposure Speckle Imaging technique, we were able to accurately estimate large changes in blood flow in the brain, such as one caused by a severe ischemic stroke. Additionally, using the Multi Exposure

#127521 - $15.00 USD Received 26 Apr 2010; revised 28 Jun 2010; accepted 1 Jul 2010; published 16 Jul 2010

Speckle Imaging technique, we were able to image through a thinned yet intact skull, and obtain consistent and accurate measures of changes in cerebral blood flow. These developments should improve the quantitative accuracy of cerebral blood flow images. Also, the ability to quantitatively image through the skull will give researchers more freedom to design chronic and long term studies of ischemic strokes.

Acknowledgments

This work was funded by grants from the American Heart Association (0735136N), the National Science Foundation (CBET/0737731), the Coulter Foundation and the Dana Foundation.

#127521 - $15.00 USD Received 26 Apr 2010; revised 28 Jun 2010; accepted 1 Jul 2010; published 16 Jul 2010